JOC Article
pubs.acs.org/joc

Synthesis and Photochemical Properties of 12-Substituted versus 13-Substituted Chlorins

Olga Mass,[†] Marcin Ptaszek,[†] Masahiko Taniguchi,[†] James R. Diers,[‡] Hooi Ling Kee,[§] David F. Bocian,*[,‡] Dewey Holten,*[,§] and Jonathan S. Lindsey*[,†]

[†]*Department of Chemistry, North Carolina State University, Raleigh, North Carolina 27695-8204,* [‡]*Department of Chemistry, University of California, Riverside, California 92521-0403, and* [§]*Department of Chemistry, Washington University, St. Louis, Missouri 63130-4889*

david.bocian@ucr.edu; holten@wuchem.wustl.edu; jlindsey@ncsu.edu

Received April 3, 2009

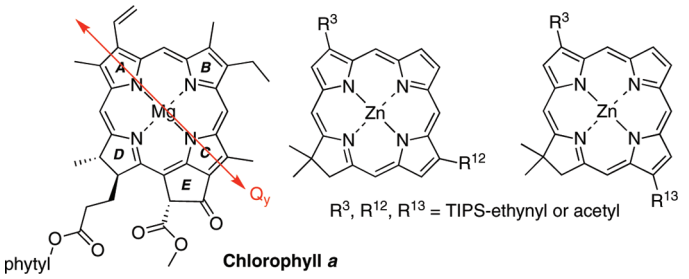

Chlorophyll *a*

Understanding the effects of substituents on natural photosynthetic pigments is essential for the rational design of artificial photosynthetic systems. The long-wavelength absorption of chlorins derives from a transition that encompasses rings A and C, which includes the 2,3- and 12,13-positions, respectively. Chlorophylls bear a 3-vinyl group and a 13-keto group, as well as a full complement of substituents at the other β-pyrrole sites. Prior studies of sparsely substituted synthetic chlorins to probe the effects of substituents yielded 3,13-substituted chlorins that contain a geminal dimethyl group in the pyrroline ring (for stability) and a mesityl group at the 10-position. Attempts to prepare analogous chlorins lacking the 10-mesityl substituent encountered unexpected difficulties during construction of the Eastern half precursor (8,9-dibromo-1-formyldipyrromethane) to the 13-bromochlorin. Direct bromination of 1-formyldipyrromethane with 2 mol equiv of NBS at −78 °C led to an isomeric mixture of the desired 8,9-dibromodipyrromethane (minor) and the unexpected 7,9-dibromodipyrromethane (major). Hence, a new rational route was developed for the synthesis of 8,9-dibromo-1-formyldipyrromethane that entailed (i) $InCl_3$-catalyzed condensation of 4-bromo-2-(hydroxymethyl)pyrrole and pyrrole to give the 8-bromodipyrromethane, (ii) 1-formylation, and (iii) 9-bromination. Two new substituted chlorins carrying auxochromes at the 3- and 13-positions were synthesized. The photophysical and redox properties of the 13-substituted chlorins were compared with those of isomeric 12-substituted chlorins, synthesized previously via a 7,9-dibromo-1-formyldipyrromethane. Such studies (static absorption and fluorescence spectroscopy, time-resolved fluorescence spectroscopy, electrochemistry of the zinc chelates, and density functional theoretical calculations) reveal only very slight differences between the isomeric 12- and 13-substituted chlorins.

Introduction

Understanding the effects of substituents on the spectral properties of chlorophyll molecules is of fundamental importance. Knowledge gained from such studies also enables subtle tuning of the absorption bands of chlorins, which is of interest for application in solar energy conversion[1] as well as diverse biomedical fields such as polychromatic flow cytometry,[2] molecular imaging,[3] and photodynamic therapy.[4] In this regard, synthetic macrocycles that contain the chlorin

(1) Stromberg, J. R.; Marton, A.; Kee, H. L.; Kirmaier, C.; Diers, J. R.; Muthiah, C.; Taniguchi, M.; Lindsey, J. S.; Bocian, D. F.; Meyer, G. J.; Holten, D. *J. Phys. Chem. C* **2007**, *111*, 15464–15478.

(2) De Rosa, S. C.; Brenchley, J. M.; Roederer, M. *Nature Med.* **2003**, *9*, 112–117.

(3) (a) Licha, K. *Top. Curr. Chem.* **2002**, *222*, 1–29. (b) Stefflova, K.; Li, H.; Chen, J.; Zheng, G. *Bioconj. Chem.* **2007**, *18*, 379–388.

(4) Nyman, E. S.; Hynninen, P. H. *J. Photochem. Photobiol. B* **2004**, *73*, 1–28.

Published on Web 06/11/2009 DOI: 10.1021/jo900706x

chromophore and that bear relatively few substituents at designated sites are essential for such studies to pinpoint the effects of specific substituents.

A general route for the de novo synthesis of chlorins is shown in Scheme 1.[5−7] The synthesis employs the condensation of an Eastern half and a Western half followed by metal-mediated oxidative cyclization. The Western half contains a geminal dimethyl group, a key design feature that stabilizes the hydroporphyrin macrocycle toward oxidation. The de novo route requires far more synthetic effort than derivatization of porphyrins or semisynthesis beginning with chlorophylls;[8−21] however, the de novo route affords greater versatility in the scope and range of substituents that can be introduced, and is well suited to the preparation of sparsely substituted chlorins. The de novo route has been

SCHEME 1

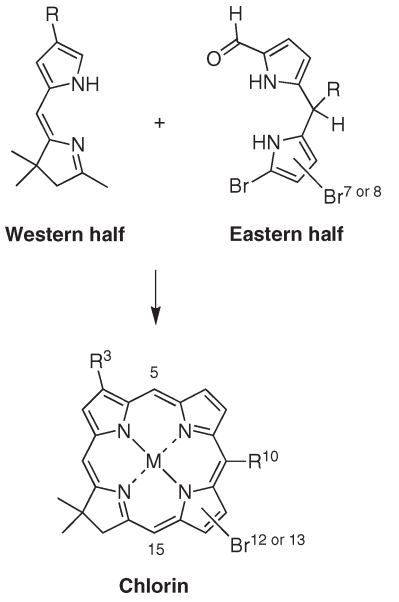

used to construct chlorins bearing a wide variety of substituents in diverse patterns.[5−7,22−35] Among various substituents and patterns, the examination of auxochromes at the 3- and 13-positions is of interest because (i) the long-wavelength absorption band of chlorophylls originates from a transition that encompasses rings A and C and (ii) chlorophylls *a* and *b* each contain auxochromes substituted in these rings, namely a 3-vinyl group and a 13-keto group.[32,36−38]

To probe the effects of auxochromes on the spectral properties of chlorins, in the past few years we have reported the synthesis of >20 chlorins that bear a 10,13-substituent pattern (and often other substituents, particularly at the 3-position),[26,27,32−35] as well as two target 3,13-substituted chlorins that lack a 10-substituent.[26] Building on the latter chemistry, we recently intended to prepare a 13-substituted chlorin that lacks a 10-substituent en route to the corresponding fully unsubstituted 13^1-oxophorbine (which, like chlorophylls, contains the 5-membered isocyclic ring spanning positions 13 and 15). However, this attempt was not successful. X-ray analysis of the putative 13-acetyl-15-bromochlorin (**ZnC-A^{13}Br^{15}**), the key intermediate for installation of the isocyclic ring, showed the acetyl group at the 12-position instead (**ZnC-A^{12}Br^{15}**; vide infra). Obviously, intramolecular α-arylation[27] of the 12-acetyl group with the

(5) Strachan, J.-P.; O'Shea, D. F.; Balasubramanian, T.; Lindsey, J. S. *J. Org. Chem.* **2000**, *65*, 3160–3172.
(6) Taniguchi, M.; Ra, D.; Mo, G.; Balasubramanian, T.; Lindsey, J. S. *J. Org. Chem.* **2001**, *66*, 7342–7354.
(7) Ptaszek, M.; McDowell, B. E.; Taniguchi, M.; Kim, H.-J.; Lindsey, J. S. *Tetrahedron* **2007**, *63*, 3826–3839.
(8) Flitsch, W. *Adv. Heterocycl. Chem.* **1988**, *43*, 73–126.
(9) Hynninen, P. H. In *Chlorophylls*; Scheer, H., Ed.; CRC Press: Boca Raton, FL, 1991; pp 145−209.
(10) Smith, K. M. In *Chlorophylls*; Scheer, H., Ed.; CRC Press: Boca Raton, FL, 1991; pp 115−143.
(11) Montforts, F.-P.; Gerlach, B.; Höper, F. *Chem. Rev.* **1994**, *94*, 327–347.
(12) Montforts, F.-P.; Glasenapp-Breiling, M. *Prog. Heterocycl. Chem.* **1998**, *10*, 1–24.
(13) Jaquinod, L. In *The Porphyrin Handbook*; Kadish, K. M., Smith, K. M., Guilard, R., Eds.; Academic Press, San Diego, CA, 2000; Vol. 1, pp 201−237.
(14) Vicente, M. G. H. In *The Porphyrin Handbook*; Kadish, K. M., Smith, K. M., Guilard R., Eds.; Academic Press: San Diego, CA, 2000; Vol. 1, pp 149−199.
(15) Pandey, R. K.; Zheng, G. In *The Porphyrin Handbook*; Kadish, K. M., Smith, K. M., Guilard R., Eds.; Academic Press: San Diego, CA, 2000; Vol. 6; pp 157−230.
(16) Montforts, F.-P.; Glasenapp-Breiling, M. *Fortschr. Chem. Org. Naturst.* **2002**, *84*, 1–51.
(17) Pavlov, V. Y.; Ponomarev, G. V. *Chem. Heterocycl. Compd.* **2004**, *40*, 393–425.
(18) Senge, M. O.; Wiehe, A.; Ryppa, C. In *Chlorophylls and Bacteriochlorophylls. Biochemistry, Biophysics, Functions and Applications*; Grimm, B., Porra, R. J., Rüdiger, W., Scheer, H., Eds.; Advances in Photosynthesis and Respiration; Springer: Dordrecht, The Netherlands, 2006; Vol. 25, pp 27−37.
(19) Fox, S.; Boyle, R. W. *Tetrahedron* **2006**, *62*, 10039–10054.
(20) Galezowski, M.; Gryko, D. T. *Curr. Org. Chem.* **2007**, *11*, 1310–1338.
(21) Silva, A. M. G.; Cavaleiro, J. A. S. In *Progress in Heterocyclic Chemistry*; Gribble, G. W., Joule, J. A., Eds.; Elsevier: Amsterdam, The Netherlands, 2008; Vol. 19, Chapter 2, pp 44−69.
(22) Balasubramanian, T.; Strachan, J.-P.; Boyle, P. D.; Lindsey, J. S. *J. Org. Chem.* **2000**, *65*, 7919–7929.
(23) Taniguchi, M.; Kim, H.-J.; Ra, D.; Schwartz, J. K.; Kirmaier, C.; Hindin, E.; Diers, J. R.; Prathapan, S.; Bocian, D. F.; Holten, D.; Lindsey, J. S. *J. Org. Chem.* **2002**, *67*, 7329–7342.
(24) Hindin, E.; Kirmaier, C.; Diers, J. R.; Tomizaki, K.-Y.; Taniguchi, M.; Lindsey, J. S.; Bocian, D. F.; Holten, D. *J. Phys. Chem. B* **2004**, *108*, 8190–8200.
(25) Taniguchi, M.; Kim, M. N.; Ra, D.; Lindsey, J. S. *J. Org. Chem.* **2005**, *70*, 275–285.
(26) Laha, J. K.; Muthiah, C.; Taniguchi, M.; McDowell, B. E.; Ptaszek, M.; Lindsey, J. S. *J. Org. Chem.* **2006**, *71*, 4092–4102.
(27) Laha, J. K.; Muthiah, C.; Taniguchi, M.; Lindsey, J. S. *J. Org. Chem.* **2006**, *71*, 7049–7052.
(28) Taniguchi, M.; Ptaszek, M.; McDowell, B. E.; Lindsey, J. S. *Tetrahedron* **2007**, *63*, 3840–3849.
(29) Taniguchi, M.; Ptaszek, M.; McDowell, B. E.; Boyle, P. D.; Lindsey, J. S. *Tetrahedron* **2007**, *63*, 3850–3863.
(30) Muthiah, C.; Ptaszek, M.; Nguyen, T. M.; Flack, K. M.; Lindsey, J. S. *J. Org. Chem.* **2007**, *72*, 7736–7749.
(31) Muthiah, C.; Taniguchi, M.; Kim, H.-J.; Schmidt, I.; Kee, H. L.; Holten, D.; Bocian, D. F.; Lindsey, J. S. *Photochem. Photobiol.* **2007**, *83*, 1513–1528.
(32) Kee, H. L.; Kirmaier, C.; Tang, Q.; Diers, J. R.; Muthiah, C.; Taniguchi, M.; Laha, J. K.; Ptaszek, M.; Lindsey, J. S.; Bocian, D. F.; Holten, D. *Photochem. Photobiol.* **2007**, *83*, 1110–1124.
(33) Muthiah, C.; Kee, H. L.; Diers, J. R.; Fan, D.; Ptaszek, M.; Bocian, D. F.; Holten, D.; Lindsey, J. S. *Photochem. Photobiol.* **2008**, *84*, 786–801.
(34) Ruzié, C.; Krayer, M.; Lindsey, J. S. *Org. Lett.* **2009**, *11*, 1761–1764.
(35) Muthiah, C.; Lahaye, D.; Taniguchi, M.; Ptaszek, M.; Lindsey, J. S. *J. Org. Chem.* **2009**, *74*, 3237–3247.
(36) Kee, H. L.; Kirmaier, C.; Tang, Q.; Diers, J. R.; Muthiah, C.; Taniguchi, M.; Laha, J. K.; Ptaszek, M.; Lindsey, J. S.; Bocian, D. F.; Holten, D. *Photochem. Photobiol.* **2007**, *83*, 1125–1143.
(37) Scheer, H. In *Chlorophylls and Bacteriochlorophylls*; Grimm, B., Porra, R. J., Rüdiger, W., Scheer, H., Eds.; Advances in Photosynthesis and Respiration; Springer: Dordrecht, The Netherlands, 2006; Vol. 25, pp 1−26.
(38) Kobayashi, M.; Akiyama, M.; Kano, H.; Kise, H. In *Chlorophylls and Bacteriochlorophylls*; Grimm, B., Porra, R. J., Rüdiger, W., Scheer, H., Eds.; Advances in Photosynthesis and Respiration; Springer: Dordrecht, The Netherlands, 2006; Vol. 25, pp 79−94.

CHART 1

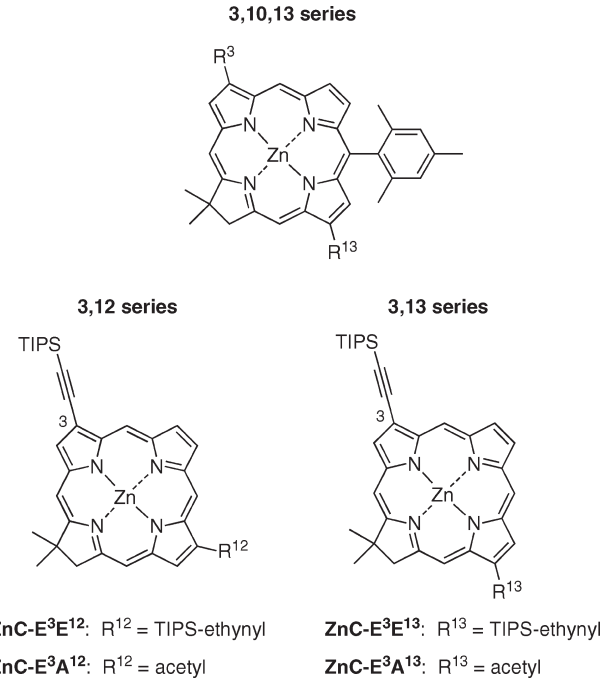

15-position cannot form the isocyclic ring. Consequently, the two target chlorins **ZnC-E^{3}E^{13}** and **ZnC-E^{3}A^{13}** (and their chlorin precursors **ZnC-Br^{3}Br^{13}** and **ZnC-E^{3}Br^{13}**) reported by us previously as 13-substituted chlorins[26] actually are the isomeric 12-substituted macrocycles **ZnC-E^{3}E^{12}** and **ZnC-E^{3}A^{12}** (and their precursors are **ZnC-Br^{3}Br^{12}** and **ZnC-E^{3}Br^{12}**), respectively (Chart 1). The structures assigned for all of the 10,13-substituted chlorins are correct.

The synthesis of the fully unsubstituted 13^1-oxophorbine remains an important objective. Because such synthesis requires the ability to prepare the 13-acetylchlorin (lacking the 10-substituent), and the prior error in assignments is restricted to the 10-unsubstituted (but not 10-substituted) chlorins,[26] we carried out a lengthy study to understand how the regiochemistry of substitution in ring C depends on the nature of the 10-substituent. The provision for introduction of substituents in ring C of the chlorin is set at the dipyrromethane stage. The dipyrromethane required for the synthesis of 13-substituted chlorins carries a 1-formyl group and two bromine atoms: the electrophilic α-carbon atom bonded with a bromine atom serves for condensation with a Western half, and the β-bromine atom in turn enables subsequent modifications at the 13-site. Thus, the 12- versus 13-substitution in the chlorins originates from a change in the regiochemistry upon introduction of the bromine atoms in the 1-formyldipyrromethane.

In this paper, we first describe the bromination of 1-formyldipyrrromethanes (which contain a 5-mesityl substituent or no 5-substituent) and characterize the brominated dipyrromethane products. Note that the 5(or meso)-position of the dipyrromethane corresponds to the 10-position of the chlorin. This study reveals an unexpected interplay of steric and electronic effects in controlling the regiochemistry of dibromination of 1-formyldipyrromethanes. We next describe a new, independent synthesis of 8,9-dibromo-1-formyldipyrromethane, which provides the critical precursor

SCHEME 2

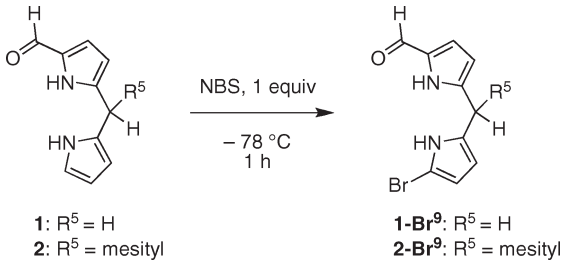

for the rational synthesis of 3,13-disubstituted chlorins and thereby overcomes the undesired regiochemistry upon dibromination of the 5-unsubstituted 1-formyldipyrromethane. The photophysical and redox properties of the resulting 3,13-disubstituted chlorins are presented and are compared with those from the previously synthesized 3,12-disubstituted chlorin isomers.[32,36] This work provides access to chlorins for fundamental studies of the effects of substituents on the spectral properties of molecules related to the chlorophylls. This work also sets the stage for extension to the fully unsubstituted 13^1-oxophorbine, which will be described in due course.

Results and Discussion

I. Bromination of Dipyrromethanes. Many studies have been reported concerning the bromination of pyrroles,[39] and bromo-substituted dipyrrins (the oxidized counterparts of dipyrromethanes) have longstanding use in classical porphyrin syntheses.[40] On the other hand, the bromination of dipyrromethanes has been less extensively investigated, particularly where nearly all pyrrole positions are open.[41] Introduction of bromine atoms in dipyrromethanes plays an important role in the synthesis of Eastern halves for the preparation of substituted chlorins. We reported previously that bromination of 1-formyldipyrromethanes lacking a 5-substituent (**1**) or containing a 5-substituent (**2**) with 1 mol equiv of NBS at −78 °C proceeded to the 9-position, affording **1-Br^9** and **2-Br^9**, respectively.[26] This result was expected (and confirmed here as shown in Scheme 2) given the deactivation of the α-formyl-substituted pyrrole ring, and the known course of electrophilic aromatic substitution of 2-alkylpyrroles.[42] On the other hand, we report here that bromination of 1-formyldipyrromethanes with 2 mol equiv of NBS proceeds with a more subtle outcome: the site of the second bromination depends on the nature of the 5-substituent (R^5 in Scheme 2). The key results are described below.

The bromination of 1-formyldipyrromethanes[43] **1** and **2** was carried out with 2 mol equiv of NBS under the same conditions applied previously[26] (2 mol equiv of NBS at

(39) Artico, M. In *Pyrroles. Part One*; Jones, R. A., Ed.; John Wiley & Sons, Inc.: New York, 1990; pp 329−395.
(40) (a) Fischer, H.; Orth, H. *Die Chemie Des Pyrroles*; Johnson Reprint Corp.: New York, 1968; Vol. II, First Half. (b) Smith, K. M. In *Porphyrins and Metalloporphyrins*; Smith, K. M., Ed.; Elsevier Scientific Publishing Co.: Amsterdam, The Netherlands, 1975; pp 29−58. (c) Paine, J. B. III In *The Porphyrins*; Dolphin, D., Ed.; Academic Press: New York, 1978; Vol. 1, pp 101−234.
(41) Liu, Z.; Yasseri, A. A.; Loewe, R. S.; Lysenko, A. B.; Malinovskii, V. L.; Zhao, Q.; Surthi, S.; Li, Q.; Misra, V.; Lindsey, J. S.; Bocian, D. F. *J. Org. Chem*. **2004**, *69*, 5568–5577.
(42) Thamyongkit, P.; Bhise, A. D.; Taniguchi, M.; Lindsey, J. S. *J. Org. Chem*. **2006**, *71*, 903–910.
(43) Ptaszek, M.; McDowell, B. E.; Lindsey, J. S. *J. Org. Chem*. **2006**, *71*, 4328–4331.

SCHEME 3

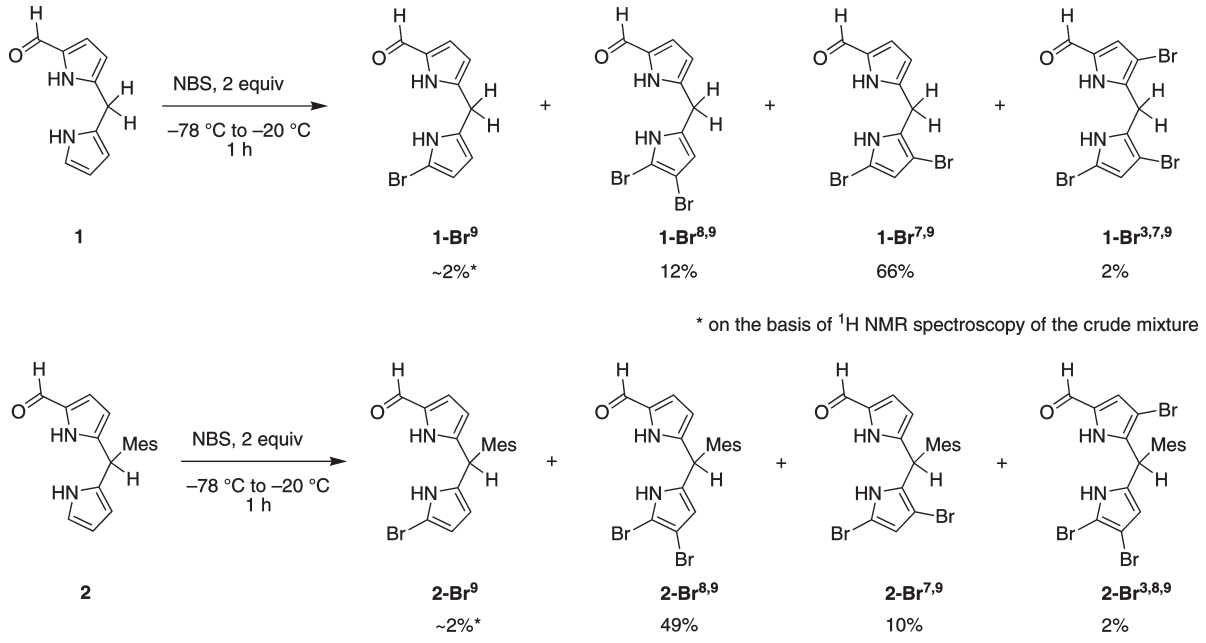

−78 through −20 °C). The results are shown in Scheme 3. The bromination of 5-unsubstituted dipyrromethane **1** afforded the isomeric dibromodipyrromethanes **1-Br^{8,9}** and **1-Br^{7,9}** in the ratio 1:5, as well as trace quantities of the monobrominated dipyrromethane **1-Br^{9}** and the unstable tribrominated dipyrromethane **1-Br^{3,7,9}** (estimated 80% isolated purity). The two dibromodipyrromethane isomers were separable upon column chromatography [silica, hexanes/CH_2Cl_2/ethyl acetate (7:2:1)], where dibromodipyrromethane **1-Br^{7,9}** was less polar than its isomer **1-Br^{8,9}**. To ensure that the isolated yields were not biased by selective loss upon workup, the ratio of dibromodipyrromethane isomers was determined on the basis of ^{1}H NMR spectroscopy of the crude mixture, relying on the noticeable difference in chemical shifts of the pyrrolic protons of the pair of dibromodipyrromethane isomers (**1-Br^{8,9}** and **1-Br^{7,9}**; Figure 1). The ratio of the pair of isomers was essentially identical in the crude reaction mixture as upon isolation in pure form. In summary, the dibromodipyrromethane previously assigned[26] as the 8,9-dibromo isomer actually is the 7,9-dibromo isomer **1-Br^{7,9}**.

This result prompted us to repeat the very bromination of 5-mesityldipyrromethane **2** described earlier.[26] Thus, bromination of 5-mesityldipyrromethane **2** under the same conditions led to the isomeric dibromodipyrromethanes **2-Br^{8,9}** and **2-Br^{7,9}** in the ratio 5:1, as well as very small amounts of monobromodipyrromethane **2-Br^{9}** and unstable tribromodipyrromethane **2-Br^{3,8,9}** (Scheme 3). 7,9-Dibromodipyrromethane **2-Br^{7,9}** also was less polar than its isomer, 8,9-dibromopyrromethane **2-Br^{8,9}**, and the two dibromodipyrromethanes were readily isolated (although **2-Br^{7,9}** and **2-Br^{3,8,9}** were isolated in estimated 90% purity). Finally, an analogous bromination study of 1-formyl-5-phenyldipyrromethane resulted in a 5:1 ratio of the 8,9-dibromo versus 7,9-dibromodipyrromethane product (see Supporting Information), indicating that the 5-phenyl substituent caused the same regiochemical outcome as the 5-mesityl substituent.

This study demonstrates that the regioselectivity of bromination is affected by the steric bulk of the 5-substituent. The first bromination occurs at the 9-position for both **1** and **2**. In the case of 9-bromo-1-formyldipyrromethane (**1-Br^{9}**), both positions C-7 and C-8 are sterically accessible for the second bromination. Position 7 is flanked by the bridging $-CH_2-$ and H^8; position 8 is flanked by the 9-bromine substituent and H^7. Consequently, the second bromination occurs preferentially at the 7-position (giving **1-Br^{7,9}**). On the other hand, the CPK projection of 9-bromodipyrromethanes (analogues of **1-Br^{9}** lacking the 1-formyl group) shows how the bulky 5-substituent hinders the 7-position (Figure 2), thereby explaining the major direction of the second bromination in this case to the less sterically shielded 8-position (giving **2-Br^{8,9}**).

II. Synthesis. A. 12-Acetylchlorin. The 5-unsubstituted 7,9-dibromodipyrromethane **1-Br^{7,9}** (interpreted previously as an 8,9-dibromodipyrromethane[26]) was synthesized at the preparative level under the same conditions as in the previous work.[26] Full characterization by a number of two-dimensional NMR experiments (HH-COSY, NOESY, and TOCSY) confirmed the position of the bromine atoms at positions 7 and 9. Dibromodipyrromethane **1-Br^{7,9}** was condensed with Western half[44] **3** in CH_2Cl_2 upon treatment with a solution of $TsOH \cdot H_2O$ in MeOH followed by Zn(II)-mediated oxidative cyclization with 2,2,6,6-tetramethylpiperidine, $Zn(OAc)_2$, and AgOTf open to air.[7,30] Chlorin **H_2C-Br^{12}** was obtained in 8% yield. Acetylation can be achieved by Pd-mediated coupling with tributyl(1-ethoxyvinyl)tin[45] followed by acidic hydrolysis. Previously we used THF for such reactions.[26,27,30,32,46] New conditions developed recently for hydroporphyrin acetylation [CH_3CN/DMF (3:2), C. Ruzié and J. S. Lindsey, unpublished data]

(44) Ptaszek, M.; Bhaumik, J.; Kim, H.-J.; Taniguchi, M.; Lindsey, J. S. *Org. Process Res. Dev.* **2005**, *9*, 651–659.
(45) Kosugi, M.; Sumiya, T.; Obara, Y.; Suzuki, M.; Sano, H.; Migita, T. *Bull. Chem. Soc. Jpn.* **1987**, *60*, 767–768.
(46) Taniguchi, M.; Cramer, D. L.; Bhise, A. D.; Kee, H. L.; Bocian, D. F.; Holten, D.; Lindsey, J. S. *New J. Chem.* **2008**, *32*, 947–958.

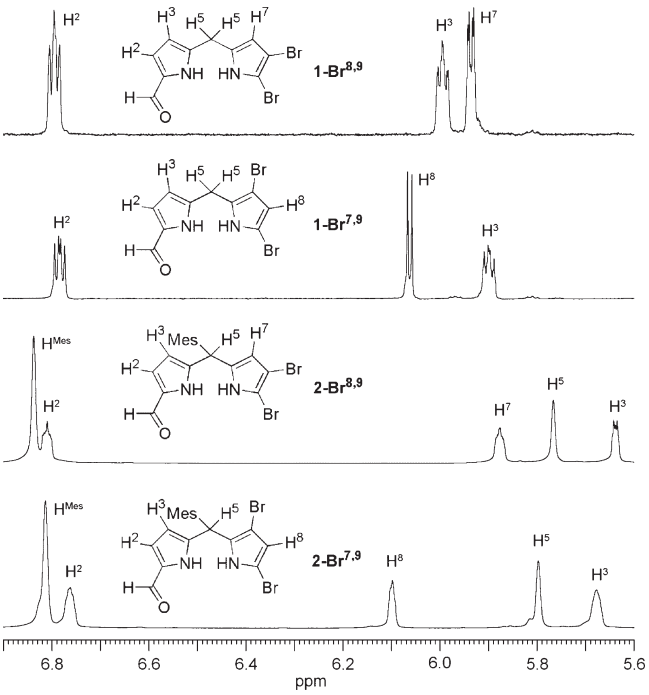

FIGURE 1. ^{1}H NMR spectra showing diagnostic features for 7, 9- versus 8,9-dibromodipyrromethanes.

afford shorter reaction time (2.5 versus 20 h) with comparable if not increased yield. Application of such conditions afforded **H$_2$C-A^{12}** in 78% yield. Metalation of **H$_2$C-A^{12}** readily afforded the zinc chelate **ZnC-A^{12}**. Chlorin **H$_2$C-A^{12}** was subjected to regioselective bromination (under acidic conditions[35]) at the 15-position to give **H$_2$C-A^{12}Br^{15}** in 40% yield (Scheme 4). Two-dimensional NMR experiments of both **H$_2$C-Br^{12}** and **H$_2$C-A^{12}Br^{15}**, and X-ray analysis of **H$_2$C-A^{12}Br^{15}**, confirmed the structures of each chlorin (see the Supporting Information), and, therefore, the position of bromine atoms at positions 7 and 9 in the chlorin precursor, namely dipyrromethane **1-Br^{7,9}**.

B. 8,9-Dibromo-1-formyldipyrromethane. To overcome the undesired regiochemical outcome upon dibromination of 1-formyldipyrromethane **1**, we developed a stepwise synthesis of 8,9-dibromodipyrromethane **1-Br^{8,9}**. The stepwise synthesis relies on a sequence of formylation and bromination where each newly introduced substituent provides regioselectivity for the next reaction (Scheme 5). The synthesis begins with 4-bromopyrrole-2-carboxaldehyde (**4**).[26] Reduction of **4** with $NaBH_4$ in THF/MeOH (10:1) afforded the corresponding carbinol **4-OH**, which was subjected to solventless condensation with pyrrole (20 mol equiv versus **4**) in the presence of a mild Lewis acid ($InCl_3$) to give 5-unsubstituted 8-bromodipyrromethane **5** in 58% yield. Attempts to purify **5** by crystallization were unsuccessful. Purification by column chromatography afforded **5** as a colorless oil that was fully characterized, although the oil darkened quickly and decomposed upon long-term storage. Dipyrromethane **5** was previously obtained in a similar manner but with HCl catalysis, and was not fully characterized.[30] A number of prior stepwise

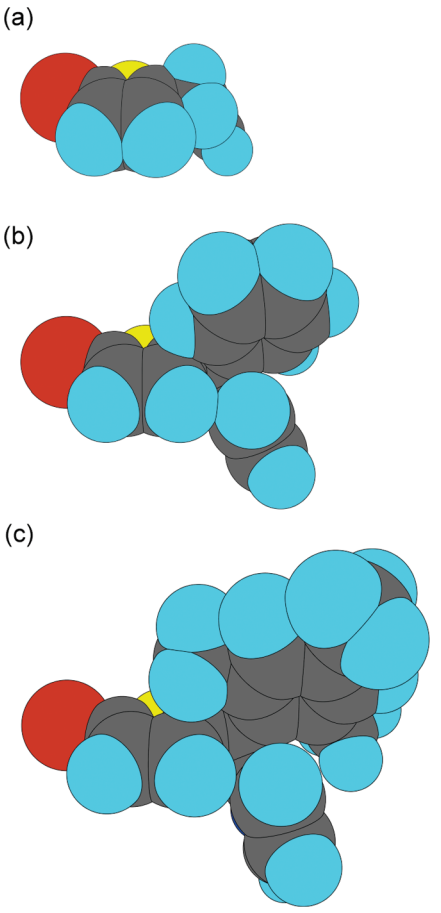

FIGURE 2. Optimized structures of 9-bromodipyrromethanes with MM2 (CPK projection). The 1-formyl group was omitted in the calculations. In each structure, the 9-bromine atom is shown at left in red, and nitrogen is shown in yellow. 9-Bromodipyrromethane (a) shows little or no steric differentiation of the 7- and 8-positions toward bromination whereas for 9-bromo-5-phenyldipyrromethane (b) and 9-bromo-5-mesityldipyrromethane (c) the steric effect of the 5-aryl substituent suppresses bromination at the neighboring 7-position.

syntheses of sparsely substituted dipyrromethanes have employed a similar approach, often with the use of protective groups.[22,42,47−53]

The standard Vilsmeier−Haack formylation[54] of **5** afforded 1-formyl-8-bromodipyrromethane **1-Br^8** in 40% yield. Protection of the pyrrolic nitrogen atom to direct the formylation to the 1-position is not required: the 8-bromine atom deactivates the adjacent 9-position, and formylation proceeded regioselectively at the most active site in the dipyrromethane, namely the 1-position. Treatment of **1-Br^8** with 1 mol equiv of NBS at −78 °C afforded 8,9-dibromodipyrromethane **1-Br^{8,9}** as the major product in 71% yield.

(47) Wallace, D. M.; Leung, S. H.; Senge, M. O.; Smith, K. M. *J. Org. Chem.* **1993**, *58*, 7245–7257.
(48) Lee, C.-H.; Lindsey, J. S. *Tetrahedron* **1994**, *50*, 11427–11440.
(49) Noss, L.; Liddell, P. A.; Moore, A. L.; Moore, T. A.; Gust, D. *J. Phys. Chem. B* **1997**, *101*, 458–465.
(50) Abell, A. D.; Nabbs, B. K.; Battersby, A. R. *J. Org. Chem.* **1998**, *63*, 8163–8169.
(51) Cho, W.-S.; Kim, H.-J.; Littler, B. J.; Miller, M. A.; Lee, C.-H.; Lindsey, J. S. *J. Org. Chem.* **1999**, *64*, 7890–7901.
(52) Littler, B. J.; Miller, M. A.; Hung, C.-H.; Wagner, R. W.; O'Shea, D. F.; Boyle, P. D.; Lindsey, J. S. *J. Org. Chem.* **1999**, *64*, 1391–1396.
(53) Balasubramanian, T.; Lindsey, J. S. *Tetrahedron* **1999**, *55*, 6771–6784.
(54) Dogutan, D. K.; Ptaszek, M.; Lindsey, J. S. *J. Org. Chem.* **2007**, *72*, 5008–5011.

SCHEME 4

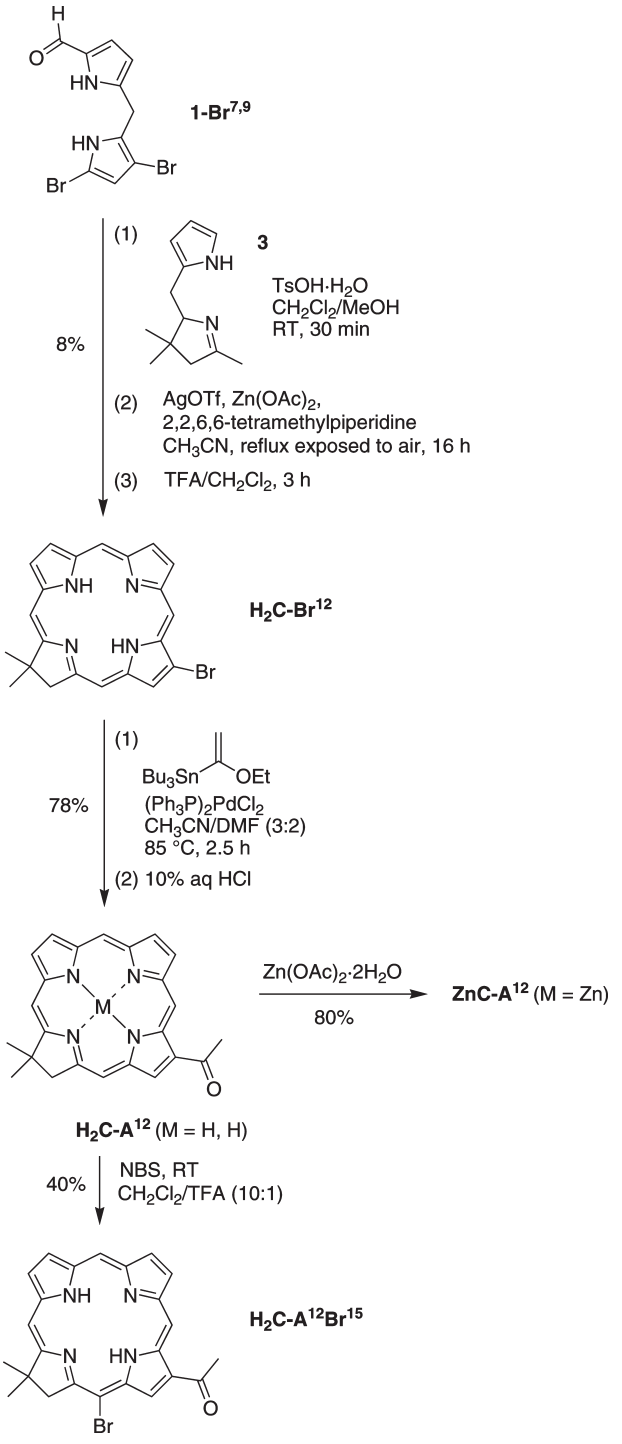

Here, the deactivation caused by the 1-formyl group prevents bromination at the 2- and 3-positions. Dipyrromethane **1-Br^{8,9}** was crystalline, thus allowing purification without use of column chromatography. The regioselectivity of bromination was established by NMR spectroscopy (HH-COSY and NOESY experiments, see the Supporting Information). Compound **1-Br^{8,9}** can be stored in solid form at 4 °C for at least 10 weeks without decomposition.

C. 3,13-Substituted Chlorins. Two 3,13-substituted chlorins bearing auxochromes were synthesized by using the newly synthesized 8,9-dibromodipyrromethane **1-Br^{8,9}**. Thus, the reaction of the Eastern half **1-Br^{8,9}** with the Western half bearing a bromine substituent (**6**)[26] was carried out in the standard way,[7,30] affording chlorin **ZnC-Br^{3}Br^{13}** in 9% yield. Sonogashira coupling with (triisopropylsilyl)acetylene in the presence of $Pd_2(dba)_3$, P(*o*-tol)$_3$, and triethylamine afforded the bis(ethynyl)chlorin **ZnC-E^{3}E^{13}** in 35% yield (Scheme 6).

SCHEME 5

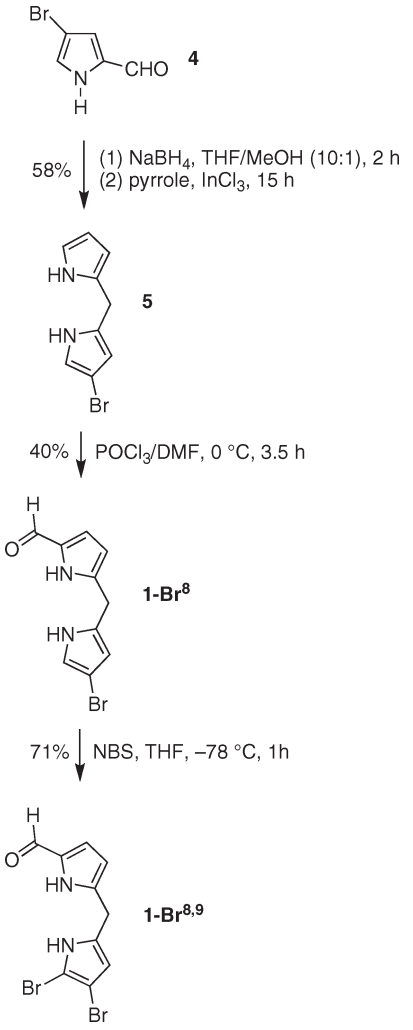

A chlorin bearing a 3-ethynyl and 13-acetyl group was prepared as shown in Scheme 7. Eastern half **1-Br^{8,9}** was condensed with ethynyl-substituted Western half **7**[26] in CH_2Cl_2 upon treatment with a solution of TsOH·H_2O in MeOH (Scheme 7). The yield upon oxidative cyclization under conventional heating did not exceed 2%, whereas microwave irradiation afforded the target chlorin **ZnC-E^{3}Br^{13}** in 5% yield. The Pd-mediated acetylation of **ZnC-E^{3}Br^{13}** was carried out in four steps including demetalation of the zinc chelate in TFA/CH_2Cl_2, acetylation under conditions analogous to those used in the preparation of **H$_2$C-A^{13}**, acidic hydrolysis in 10% aqueous HCl, and metalation with $Zn(OAc)_2 \cdot 2H_2O$. In this manner, chlorin **ZnC-E^{3}A^{13}** was obtained in 59% yield.

III. Chemical Characterization. The chlorins were characterized by ^{1}H NMR spectroscopy (including NOESY), ^{13}C NMR spectroscopy (for 3,13-disubstituted chlorins), matrix-assisted laser desorption mass spectrometry (using a matrix

SCHEME 6

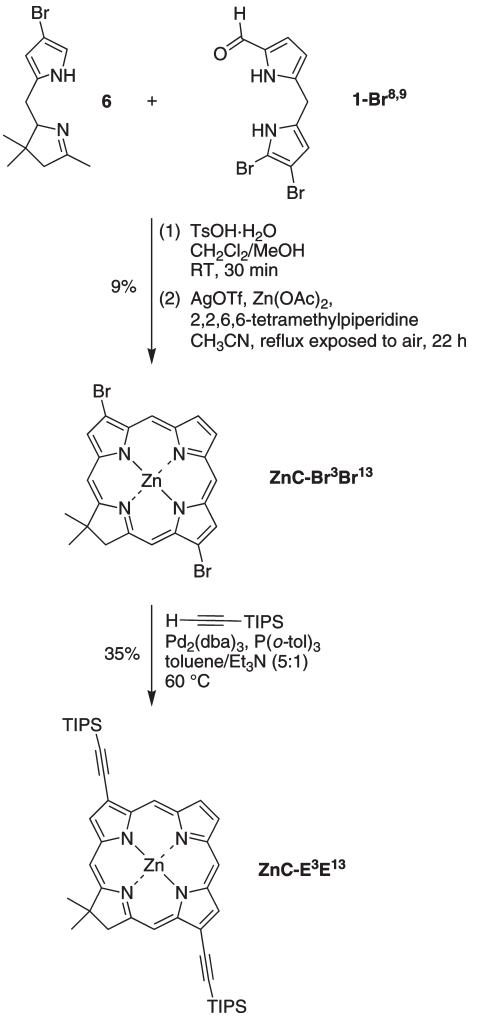

SCHEME 7

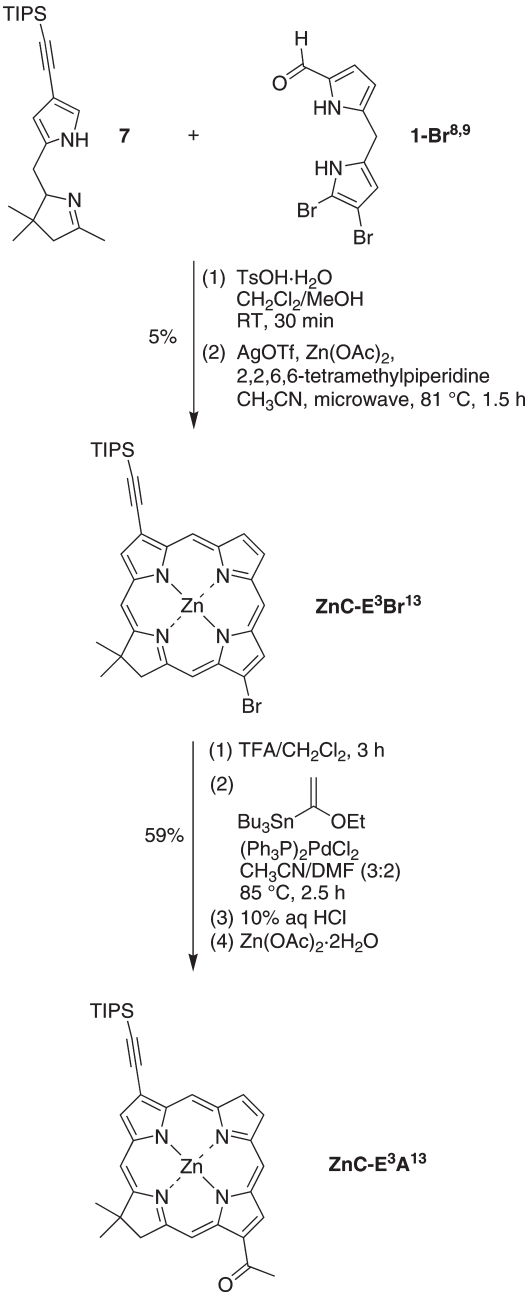

of 1,4-bis(5-phenyloxazol-2-yl)benzene),[55] high-resolution electrospray ionization mass spectrometry, and absorption and fluorescence spectroscopy.[56,57]

X-ray structures of a number of chlorins were obtained to verify the substitution patterns described herein as well as several other patterns described previously (Chart 2). Chlorin **H_2C-A^{12}Br^{15}** was prepared via the 5-unsubstituted dipyrromethane **1-Br^{7,9}**; the product and precursor were previously ascribed (incorrectly)[26] to chlorin isomer **H_2C-A^{13}Br^{15}** and dipyrromethane isomer **1-Br^{8,9}**, respectively. Chlorin **ZnC-Br^{3}Br^{13}** was prepared from 5-unsubstituted dipyrromethane **1-Br^{8,9}**; the X-ray structure thus confirms the integrity of the substitution pattern for the new synthetic route to 8,9-dibromodipyrromethanes. Additional X-ray structures of two chlorins (**ZnC-M^{10}Br^{13}**, **ZnC-T^{5}M^{10}A^{13}**) and an oxophorbine (**H_2OP-T^{5}M^{10}**) confirm the pattern of 10,13-, 5,10,13-, and 5,10,13,15-substituents, respectively (see the Supporting Information). The X-ray structure of the copper chelate **CuT^{5}M^{10}A^{13}** has been published.[27] Each of these macrocycles was prepared previously[26,27] via the intermediacy of a 5-mesityldipyrromethane that bears the 8,9-dibromo substitution pattern, thus confirming the integrity of the 8,9-dibromination of the 5-mesityldipyrromethane. Other X-ray structures of chlorins have validated the reported substitution at the 7-chlorin position.[30]

IV. Spectroscopy. A. Optical Spectra. The electronic ground state absorption spectra of **ZnC-E^{3}E^{13}** and **ZnC-E^{3}E^{12}** are shown in Figure 3, panels A and B, respectively. The longest wavelength absorption feature for each compound is the $Q_y(0,0)$ band and corresponds to the $S_0 \rightarrow S_1$ transition. This band lies at a slightly longer wavelength for **ZnC-E^{3}E^{12}** than **ZnC-E^{3}E^{13}** (645 versus 643 nm). An analogous but slightly larger shift is observed for the

(55) Srinivasan, N.; Haney, C. A.; Lindsey, J. S.; Zhang, W.; Chait, B. T. *J. Porphyrins Phthalocyanines* **1999**, *3*, 283–291.
(56) Li, F.; Gentemann, S.; Kalsbeck, W. A.; Seth, J.; Lindsey, J. S.; Holten, D.; Bocian, D. F. *J. Mater. Chem.* **1997**, *7*, 1245–1262.
(57) Kee, H. L.; Kirmaier, C.; Yu, L.; Thamyongkit, P.; Youngblood, W. J.; Calder, M. E.; Ramos, L.; Noll, B. C.; Bocian, D. F.; Scheidt, W. R.; Birge, R. R.; Lindsey, J. S.; Holten, D. *J. Phys. Chem. B* **2005**, *109*, 20433–20443.

CHART 2

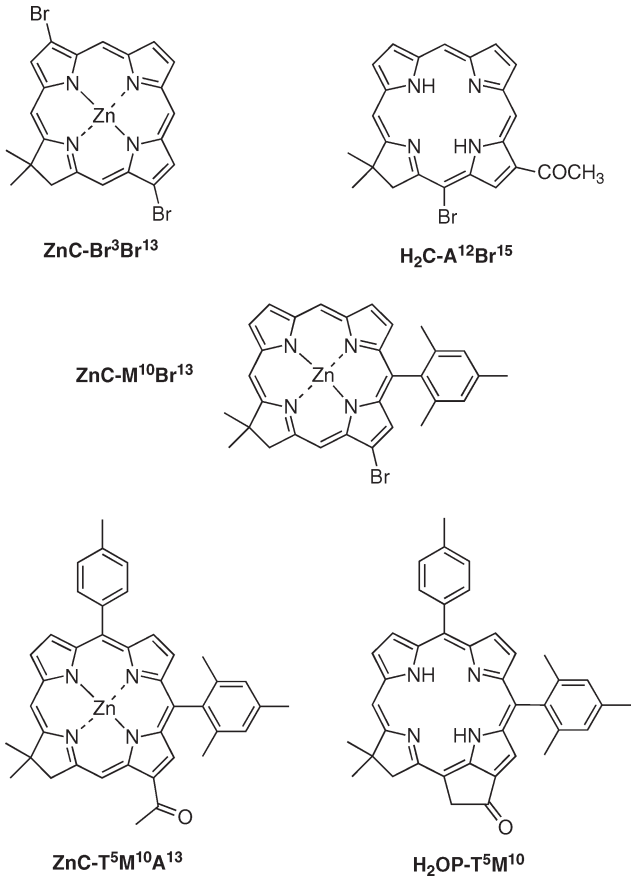

near-UV Soret feature, which corresponds to a transition from S_0 to a higher singlet excited state. Both the $Q_y(0,0)$ and Soret maxima for **ZnC-E^{3}A^{12}** are also bathochromically shifted from those for **ZnC-E^{3}A^{13}** (Figure 4), and the shifts are 2 to 4 times larger than that found for **ZnC-E^{3}E^{12}** versus **ZnC-E^{3}E^{13}**. These results also show that incorporation of the acetyl group in place of the ethynyl group at either the 12- or 13-position results in a shift of the Q_y and Soret absorption features to longer wavelengths compared to the unsubstituted chlorin (Table 1), in keeping with our prior studies of synthetic chlorins.[32,36] The ratios of the peak intensities of the Soret and Q_y bands are essentially the same for ethyne or acetyl at the 12- or 13-positions, and the same is true for the integrated intensities of the band contours (Table 1).

The $Q_y(0,0)$ $S_1 \rightarrow S_0$ fluorescence feature for each chlorin is shown in Figures 3 and 4. For each compound, there is very little Stokes shift from the corresponding absorption maximum. This finding is in accord with prior results on a large series of synthetic chlorins, indicating very little change in structural or electronic characteristics of the chlorin macrocycle following excitation. The average Stokes shift for the two acetyl-substituted chlorins **ZnC-E^{3}A^{13}** and **ZnC-E^{3}A^{12}** ($\sim$50 cm^{-1}) is larger than that for the ethynyl-substituted analogues **ZnC-E^{3}E^{13}** and **ZnC-E^{3}E^{12}** ($\sim$25 cm^{-1}). This difference may reflect in part rotation of the acetyl group with respect to the macrocycle in the excited state; however, given the small magnitudes of the shifts for both substituents, this effect is not substantial.

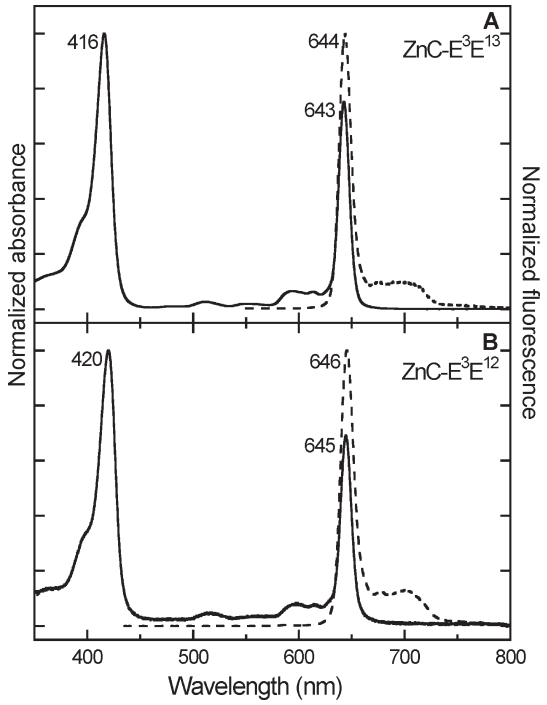

FIGURE 3. Absorption and fluorescence spectra of **ZnC-E^{3}E^{13}** (A) and **ZnC-E^{3}E^{12}** (B) in toluene. The peak wavelengths (nm) are indicated.

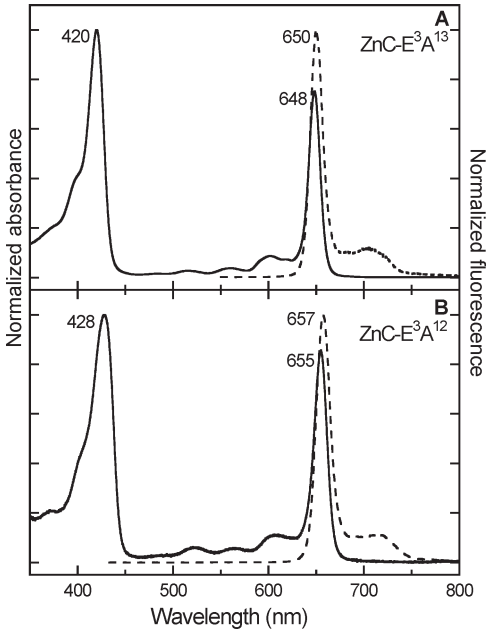

FIGURE 4. Absorption and fluorescence spectra of **ZnC-E^{3}A^{13}** (A) and **ZnC-E^{3}A^{12}** (B) in toluene. The peak wavelengths (nm) are indicated.

B. Fluorescence Quantum Yields and Excited-State Lifetimes. The fluorescence quantum yields (Φ_f) and singlet excited-state lifetimes (τ_S) for the four substituted chlorins are given in Table 1 along with the values for the parent chlorin **ZnC** (lacking any meso or β-pyrrole substituents). The incorporation of an ethynyl substituent at the 13-position of **ZnC-E^{3}E^{13}** versus the 12-position of **ZnC-E^{3}E^{12}** gives

modestly larger values for Φ_f (0.23 versus 0.18) and τ_S (3.7 ns versus 3.1 ns). Similar results are obtained for the analogous acetyl derivatives **ZnC-E^{3}A^{13}** versus **ZnC-E^{3}A^{12}**: $\Phi_f = 0.24$ versus 0.22 and $\tau_S = 4.6$ ns versus 4.1 ns. Insights into the origins of these differences can be seen from the common dependence of both Φ_f and τ_S on the rate constants for $S_1 \rightarrow S_0$ spontaneous fluorescence (k_f), $S_1 \rightarrow S_0$ internal conversion (k_{ic}), and $S_1 \rightarrow T_1$ intersystem crossing (k_{isc}) via eqs 1 and 2.

$$\tau_S = (k_f + k_{ic} + k_{isc})^{-1} \quad (1)$$

$$\Phi_f = k_f/(k_f + k_{ic} + k_{isc}) \quad (2)$$

Equation 3 shows how the radiative (fluorescence) rate constant is calculated from the measured values of Φ_f and τ_S (Table 1).

$$k_f = \Phi_f/\tau_S \quad (3)$$

The calculated k_f values are essentially the same for **ZnC-E^{3}E^{12}** and **ZnC-E^{3}E^{13}** [$(16\ ns)^{-1}$ and $(17\ ns)^{-1}$, respectively] and the same is true for **ZnC-E^{3}A^{13}** and **ZnC-E^{3}A^{12}** [both $(19\ ns)^{-1}$]. This finding, when factored into eqs 1 and 2, indicates that the greater Φ_f and τ_S values that result from placement of either an ethyne or acetyl at the 13- versus 12-position must derive from a decrease in one or both of the nonradiative rate constants (k_{ic}, k_{isc}). The energy-gap law would predict a slightly smaller internal-conversion rate constant for analogous 13- versus 12-substituted chlorins because the former compounds have a slightly greater S_1 excited state energy (as seen by the $Q_y(0,0)$ absorption and emission wavelengths, Table 1). Because k_{isc} typically dominates over k_{ic} for chorins,[32] and given that 13- versus 12-substituted chlorins exhibit slightly larger Φ_f and τ_S values, it is likely that the k_{isc} values are also smaller when an ethyne or acetyl group is placed at the 13-position compared to the 12-position. A possible underlying cause of this effect is that an ethyne or acetyl at the 13-position results in a slightly greater extent of electron delocalization off the macrocycle compared to the same group located at the 12-position.

TABLE 1. Photophysical Properties of Zinc Chlorins[a]

		$\lambda_{Q_y(0,0)}$ (nm)						
compd[b]	λ_B (nm)	absn	emis	I_B/I_{Q_y}[c]	Σ_B/Σ_{Q_y}[d]	Φ_f	τ_s (ns)	k_f^{-1} (ns)
ZnC[e]	398	602	602	3.4	4.1	0.062	1.7	27
ZnC-E^{3}E^{12}[f]	420	645	646	1.5	2.2	0.18	3.1	17
ZnC-E^{3}E^{13}	416	643	644	1.3	2.2	0.23	3.7	16
ZnC-E^{3}A^{12}[g]	428	655	657	1.2	2.0	0.22	4.1	19
ZnC-E^{3}A^{13}	420	648	650	1.3	2.2	0.24	4.6	19

[a] All samples were measured at room temperature in toluene. [b] For nomenclature, see text and Chart 1. [c] Ratio of the peak intensities of the B and $Q_y(0,0)$ bands. [d] Ratio of the integrated intensities of the B (B_x plus B_y components) and Q_y absorption manifolds, which includes the (0,0) and (1,0) features. [e] From ref 32. [f] From ref 32 wherein the compound was initially assigned as **ZnC-E^{3}E^{13}**. [g] From ref 32 wherein the compound was initially assigned as **ZnC-E^{3}A^{13}**.

C. Electrochemistry. The incorporation of two ethyne groups to the parent chlorin **ZnC** causes a significant (~0.1 V) shift of the first oxidation potential to more positives values (Table 2); furthermore, with the first ethyne at the 3-position, the $\Delta E_{1/2}^{ox}$ value is effectively the same whether the second ethyne group is located at the 12- versus 13-position (+0.40 V versus +0.41 V). Basically the same is true for 3-ethynylchlorins in which an acetyl group is placed at the 12- or 13-position (+0.42 V or +0.44 V). Turning to the first reduction potentials, the incorporation of two ethynyl groups causes a substantial (~0.25 V) shift to less negative values; furthermore, with the first ethyne at the 3-position, the $\Delta E_{1/2}^{red}$ value is effectively the same whether the second ethyne is located at the 12- or 13-position (−1.49 or −1.48 V). Again, the same is true for the addition of an acetyl group at the 12- or 13-position of a 3-ethynylchlorin (−1.42 or −1.41 V). Although there are insignificant differences if the second substituent (ethyne or acetyl) is added at the 12- or 13-position, the differences in reduction potentials of the ethynylacetylchlorins (**ZnC-E^{3}A^{12}** or **ZnC-E^{3}A^{13}**) are ~0.07 V less negative than those for the bis(ethynyl)chlorins (**ZnC-E^{3}E^{12}** or **ZnC-E^{3}E^{13}**); the corresponding oxidation potentials of the former complexes are only ~0.02 V more positive than those of the former. Thus, the ethynylacetylchlorins are significantly easier to reduce than the bis(ethynyl) analogues, but are only marginally harder to oxidize.

D. DFT Calculations. The results of the density functional theory calculations generally track the key redox and optical properties of the chlorins under study (Figure 5). The identical HOMO energies of **ZnC-E^{3}E^{12}** or **ZnC-E^{3}E^{13}** are in accord with the finding that the first oxidation potentials are the same to within 0.01 eV (Table 2). The identical LUMO energies of the same two bis(ethynyl)chlorins also are consistent with the finding that the first reduction potentials are the same to within 0.01 eV. The calculated HOMO of **ZnC-E^{3}A^{13}** being only 0.02 eV more negative than that for **ZnC-E^{3}A^{12}** is consistent with the measured $\Delta E_{1/2}^{ox}$ value of the former compound being only 0.02 eV more positive than that of the former, the values being within experimental error for the two compounds. Similarly, the calculated LUMO and measured $\Delta E_{1/2}^{red}$ values are the same for the two ethynylacetylchlorins to within 0.01 eV. The findings from the measured redox potentials that the ethynylacetylchlorins are perhaps slightly harder to oxidize but

TABLE 2. Redox Properties and Orbital Energies of Zinc Chlorins

	redox potential (V)[a]			orbital energy (eV)					
compd	$\Delta E_{1/2}^{ox}$	$\Delta E_{1/2}^{red}$	ΔE_{redox}[b]	HOMO-1	HOMO	LUMO	LUMO+1	ΔE_{MO}[c]	$\Delta E_{0,0}$[d]
ZnC	+0.30[e]	−1.74[e]	2.04	−5.16	−4.79	−2.12	−1.55	2.67	2.06
ZnC-E^{3}E^{12}	+0.40[f]	−1.49[f]	1.89	−5.31	−4.94	−2.43	−1.79	2.51	1.92
ZnC-E^{3}E^{13}	+0.41	−1.48	1.89	−5.32	−4.94	−2.43	−1.75	2.51	1.93
ZnC-E^{3}A^{12}	+0.42[g]	−1.42[g]	1.84	−5.36	−5.02	−2.58	−1.88	2.45	1.89
ZnC-E^{3}A^{13}	+0.44	−1.41	1.85	−5.36	−5.04	−2.57	−1.81	2.47	1.91

[a] Measured in butyronitrile/0.1 M n-Bu_4NPF_6; potentials versus $FeCp_2/FeCp_2^+ = +0.19$ V. [b] $\Delta E_{redox} = \Delta E_{1/2}^{ox} - \Delta E_{1/2}^{red}$. [c] $\Delta E_{MO} = E_{LUMO} - E_{HOMO}$. [d] $\Delta E_{0,0}$ is the energy of the lowest singlet excited state in toluene from Table 1. [e] From ref 36. [f] The oxidation and reduction potentials reported in ref 36, where the compound was assigned as **ZnC-E^{3}E^{13}**, were +0.40 and −1.51 V. [g] From ref 36 wherein the compound was initially assigned as **ZnC-E^{3}A^{13}**.

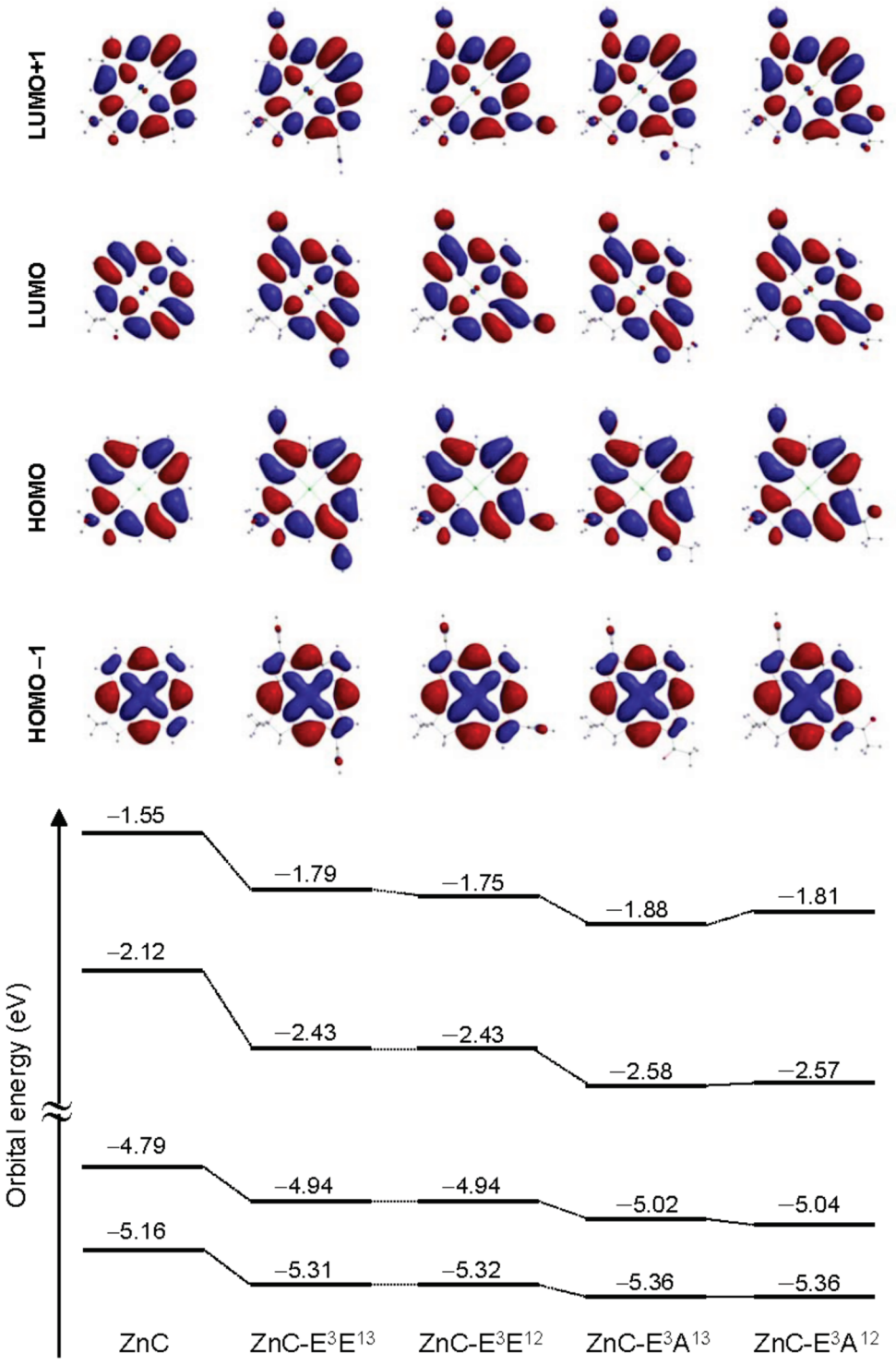

FIGURE 5. Molecular orbital energies and electron-density distributions obtained from DFT calculations.

more substantially easier to reduce are also reproduced by the differences in HOMO energies and LUMO energies, respectively. Finally, the differences in the redox properties of the four substituted chlorins with the parent chlorin **ZnC** are qualitatively reproduced by the trends in orbital energies.

The calculated orbital-energy differences $\Delta E_{MO} = E_{LUMO} - E_{HOMO}$ for **ZnC-E^{3}E^{12}** and **ZnC-E^{3}E^{13}** are the same. This result matches the finding of the same value for the measured difference in first oxidation and reduction potentials $\Delta E_{redox} = \Delta E_{1/2}^{ox} - \Delta E_{1/2}^{red}$. These two quantities in turn match the finding of the same energy ($\Delta E_{0,0}$ within 0.01 eV) of the lowest singlet excited state derived from the optical spectra. One expects the latter result since the LUMO−HOMO energy gap is a major contributor to the energy of the S_1 excited state, along with a somewhat smaller (40%) contribution from the energy gap between LUMO + 1 and

HOMO-1.[58,59] The same basic agreement is found for the ΔE_{MO}, ΔE_{redox}, and $\Delta E_{0,0}$ values for **ZnC-E^{3}A^{12}** and **ZnC-E^{3}A^{13}**. In addition, the calculated ΔE_{MO} values are slightly (~0.05 eV) smaller for the ethynylacetylchlorins than for the bis(ethynyl)chlorins, consistent with the similarly smaller experimental ΔE_{redox} and $\Delta E_{0,0}$ values for the former versus the latter chlorins.

Conclusions

Reexamination of the dibromination of dipyrromethanes **1** and **2** revealed an unexpected interplay of steric and electronic effects. In particular, the bromination of a 1-formyldipyrromethane with 2 equiv of NBS proceeds at the 9- and 7-positions when there is no steric hindrance owing to a 5-aryl substituent; in the presence of a 5-aryl substituent, bromination proceeds at the 9- and 8-positions. The 7,9-dibromination pattern provides access to 12-substituted chlorins that lack a 10-substituent.

A rational route has been developed to 8,9-dibromo-1-formyldipyrromethane (**1-Br^{8,9}**, lacking a 5-substituent), which constitutes a key precursor for 13-substituted chlorins lacking 10-substituents. Thus, chlorins bearing a single substituent at the 12-position or 13-position can now be unambiguously obtained, the former by regioselective bromination of the Eastern half precursor (1-formyldipyrromethane), the latter by a new, stepwise synthesis of 8,9-dibromo-1-formyldipyrromethane. It is essential to set the regiochemistry of bromine substitution at the dipyrromethane stage, given that the target dibromo-1-formyldipyrromethane can be separated from isomers thereof as well as from monobromo and polybromo analogues. By contrast, the corresponding chlorin isomers are not readily separable.

The availability of both 12-substituted and 13-substituted chlorins provided an opportunity to probe the distinctions caused by this change in substitution pattern. The incorporation of an ethyne or acetyl group at the 12-position versus the 13-position of a 3-ethynylchlorin results in (1) essentially the same first oxidation potential (within 0.01 eV), (2) essentially the same first reduction potential (within 0.02 eV), (3) a small blue shift in the $Q_y(0,0)$ absorption and emission bands (~2 nm for the bis(ethynyl)chlorin and ~7 nm for the ethynylacetylchlorin), (4) an increase in fluorescence yield (~30% for the bis(ethynyl)chlorin and ~10% for the ethynylacetylchlorin), and (5) an ~15% average lengthening of the lifetime of the lowest singlet excited state. The availability of chlorin isomers identical in all aspects except for the position of a substituent at the 12- or 13-position, which grew out of an effort to understand the unexpected regiochemistry of bromination of 1-formyldipyrromethanes, has provided deeper insight into the effects of substituents on the spectral, redox, and photochemical features of analogues of chlorophyll.

Experimental Section

Absorption and Fluorescence Spectroscopy. Static absorption and fluorescence measurements were performed as described previously, typically for very dilute solutions of the compounds in toluene.[56,57] Fluorescence lifetimes were obtained by using a phase modulation technique.[57] Argon-purged solutions with an absorbance of ≤0.10 at the Soret-band λ_{exc} were used for the fluorescence spectral and lifetime measurements. For fluorescence spectra, the excitation and detection monochromators typically had a band-pass of 1.5 and 3.7 nm, respectively, and spectra were obtained with use of 0.2 nm data intervals. The emission spectra were corrected for detection-system spectral response. Fluorescence quantum yields were determined for argon-purged solutions of the chlorin relative to chlorophyll *a* in benzene (Φ_f = 0.325)[60] and were corrected for solvent refractive index.

For calculation of the integrated-intensity ratio of the Soret and Q_y absorption manifolds (Σ_B/Σ_{Q_y}), the Soret region was typically integrated from the red of the origin maximum (~450 nm) to ~350 nm in order to encompass the $B_x(0,0)$, $B_y(0,0)$, $B_x(1,0)$, and $B_y(1,0)$ features. Similarly, integration of the Q_y manifold encompassed the (0,0) band and the (1,0) feature(s), but not any (2,0) contributions. For each compound, the integration range for both the B and Q_y manifolds was chosen to attempt to best capture the associated oscillator strength while minimizing contributions from absorption to higher energy electronic states (e.g., the Q_x bands in the case of the Q_y manifold).

Electrochemistry. The electrochemical measurements were made in a standard three-electrode cell with Pt working and counter electrodes and an Ag/Ag^+ reference electrode. The solvent/electrolyte was butyronitrile containing 0.1 M *n*-BuN_4PF_6. The potentials are reported versus $FeCp_2/FeCp_2^+ = 0.19$ V.

Molecular Orbital Calculations. Density functional theory (DFT) calculations were performed as described previously,[36] using the hybrid B3LYP functional and a 6-31G* basis set. The equilibrium geometry of each complex was fully optimized by using the complete structure and the default parameters of the program.

Bromination of 1-Formyldipyrromethane (1). A solution of **1** (174 mg, 1.00 mmol) in anhydrous THF (10 mL) at −78 °C was treated with NBS (348 mg, 2.00 mmol) in one batch under argon. The reaction mixture was stirred for 1 h at −78 °C, after which the ice bath was removed. A thermometer was placed in the reaction mixture. The reaction mixture was allowed to warm up. Hexanes (10 mL) and water (10 mL) were added when the temperature of the reaction mixture reached −20 °C. The entire contents of the reaction flask were transferred to a separatory funnel. Ethyl acetate (20 mL) was added. The organic layer was separated, dried (K_2CO_3), and concentrated without heating to afford a brown solid. Column chromatography [silica, hexanes/CH_2Cl_2/ethyl acetate (7:2:1)] afforded three brominated dipyrromethanes in the following order: a trace of 3,7,9-tribromo-1-formyldipyrromethane (**1-Br^{3,7,9}**, estimated 80% purity, 8 mg, 2%); a dominant amount of 7,9-dibromo-1-formyldipyrromethane (**1-Br^{7,9}**, 219 mg, 66%); and finally a lesser amount of 8,9-dibromo-1-formyldipyrromethane (**1-Br^{8,9}**, 41 mg, 12%).

The three products were examined by ^{1}H NMR spectroscopy. The ^{1}H NMR data for **1-Br^{7,9}** were consistent with those described previously (reported as **1-Br^{8,9}**).[27] The ^{1}H NMR data for **1-Br^{8,9}** were consistent with those described for the compound prepared by rational synthesis (vide infra). Compound **1-Br^{3,7,9}** has not been previously described.

Data for **1-Br^{3,7,9}**: ^{1}H NMR (THF-d_8) δ 3.96 (s, 2H), 6.06 (m, 1H), 6.92 (m, 1H), 9.37 (s, 1H), 10.71 (br s, 1H), 11.45 (br s, 1H); ESI-MS obsd 408.8184 $(M + H)^+$ corresponds to 407.81114 (M), calcd 407.81085 ($C_{10}H_7Br_3N_2O$).

Bromination of 1-Formyl-5-mesityldipyrromethane (2). Bromination of **2** (292 mg, 1.00 mmol) was carried out in exact

(58) Gouterman, M. In *The Porphyrins*; Dolphin, D., Ed.; Academic Press: New York, 1978; Vol. 3, pp 1−165.
(59) Petit, L.; Quartarolo, A.; Adamo, C.; Russo, N. *J. Phys. Chem. B* **2006**, *110*, 2398–2404.
(60) Weber, G.; Teale, F. W. J. *Trans. Faraday Soc.* **1957**, *53*, 646–655.

analogy with that of **1**. Column chromatography [silica, hexanes/CH_2Cl_2/ethyl acetate (7:2:1)] afforded three brominated dipyrromethanes in the following order: a trace of 3,8,9-tribromo-1-formyl-5-mesityldipyrromethane (**2-Br^{3,8,9}**, estimated 90% purity, 9 mg, 2%); an amount of 7,9-dibromo-1-formyl-5-mesityldipyrromethane (**2-Br^{7,9}**, estimated 90% purity, 37 mg, 10%); and finally a dominant amount of 8,9-dibromo-1-formyl-5-mesityldipyrromethane (**2-Br^{8,9}**, 180 mg, 49%). The three products were examined by ^{1}H NMR spectroscopy. The ^{1}H NMR data for **2-Br^{8,9}** were consistent with those described previously.[26] Compounds **2-Br^{7,9}** and **2-Br^{3,8,9}** have not been previously described.

Data for **2-Br^{7,9}**: mp 66−68 °C dec; ^{1}H NMR (THF-d_8) δ 2.06 (s, 6H), 2.23 (s, 3H), 5.67−5.68 (m, 1H), 5.80 (s, 1H), 6.10 (s, 1H), 6.76 (s, 1H), 6.81 (s, 2H), 9.42 (s, 1H), 10.46 (br s, 1H), 11.31 (br s, 1H); ^{13}C NMR (THF-d_8) δ 21.1, 21.2, 39.9, 96.7, 97.4, 112.0, 113.5, 121.1, 131.1, 132.0, 134.3, 135.4, 137.1, 137.9, 139.8, 178.7; ESI-MS obsd 448.98618 $(M + H)^+$ corresponds to 447.97890 (M), calcd 447.97859 ($C_{19}H_{18}Br_2N_2O$).

Data for **2-Br^{3,8,9}**: mp 65 °C dec; ^{1}H NMR (THF-d_8) δ 2.06 (s, 6H), 2.23 (s, 3 H), 5.54−5.55 (m, 1H), 5.74 (s, 1H), 6.82 (s, 2H), 6.94−6.95 (m, 1H), 9.39 (s, 1H), 11.01 (br s, 1H), 11.26 (br s, 1H); ESI-MS obsd 526.8955 $(M + H)^+$ corresponds to 525.88826, calcd 525.88910 ($C_{19}H_{17}Br_3N_2O$).

7,9-Dibromo-1-formyldipyrromethane (1-Br^{7,9}). Following the procedure for dibromination of 1-formyldipyrromethanes (described incorrectly to give **1-Br^{8,9}**),[26] a solution of **1** (174 mg, 1.00 mmol) in anhydrous THF (15 mL) at −78 °C was treated with NBS (383 mg, 2.20 mmol) in one batch under argon. The reaction mixture was stirred for 1 h at −78 °C, after which the ice bath was removed, and the reaction mixture was allowed to warm up. Hexanes was added when the reaction mixture reached −20 °C, and water was added upon reaching 0 °C. Ethyl acetate was added. The organic layer was separated, dried (K_2CO_3), and concentrated without heating to afford a brown solid. Column chromatography [silica, hexanes/CH_2Cl_2/ethyl acetate (7:2:1)] afforded a pinkish-white solid (175 mg, 52%): mp 109−111 °C dec; ^{1}H NMR (THF-d_8) δ 3.94 (s, 2H), 5.89−5.91 (m, 1H), 6.06 (m, 1H), 6.77−6.80 (m, 1H), 9.37 (s, 1H), 10.84 (br s, 1H), 11.17 (br s, 1H); ^{13}C NMR (THF-d_8) δ 96.2, 97.9, 110.0, 112.6, 121.6, 121.7, 128.8, 134.2, 138.9, 178.4. Anal. Calcd for $C_{10}H_8Br_2N_2O$: C, 36.18; H, 2.43; N, 8.44. Found: C, 36.58; H, 2.50; N, 8.11.

12-Bromo-17,18-dihydro-18,18-dimethylporphyrin (H_2C-Br^{12}). A solution of **1-Br^{7,9}** (155 mg, 0.467 mmol) and **3** (88 mg, 0.47 mmol) in anhydrous CH_2Cl_2 (12 mL) was treated with a solution of TsOH·H_2O (445 mg, 2.34 mmol) in anhydrous methanol (3 mL) under argon. The color of the reaction mixture changed immediately to orange-red. The mixture was stirred for 30 min under argon, then treated with 2,2,6,6-tetramethylpiperidine (970 μL, 5.15 mmol) and concentrated to dryness. The resulting brown solid was suspended in acetonitrile (50 mL), and 2,2,6,6-tetramethylpiperidine (1.58 mL, 9.34 mmol), $Zn(OAc)_2$ (1.29 g, 7.01 mmol), and AgOTf (360 mg, 1.40 mmol) were added. The resulting suspension was refluxed for 16 h exposed to air. The reaction mixture was filtered though a silica pad, and the filtrate was concentrated to a green solid. The solid was dissolved in CH_2Cl_2 (12 mL), and the solution was stirred and treated dropwise with TFA (280 μL, 3.60 mmol). After 3 h the reaction mixture was diluted with CH_2Cl_2 and washed (saturated aqueous $NaHCO_3$, water, and brine). The organic phase was separated, concentrated, and chromatographed [silica, CH_2Cl_2/hexanes (1:2)] to afford a green solid (15 mg, 8%): ^{1}H NMR δ −2.45 (br s, 2H), 2.06 (s, 6H), 4.64 (s, 2H), 8.96−8.99 (m, 4H), 9.06 (d, J = 3.9 Hz, 1H), 9.10 (d, J = 3.9 Hz, 1H), 9.25 (d, J = 4.7 Hz, 1H), 9.85 (s, 1H), 9.92 (s, 1H); LD-MS obsd 417.8; ESI-MS obsd 419.0869 $(M + H)^+$ corresponds to 418.0796 (M), calcd 418.0793 ($C_{22}H_{19}BrN_4$); λ_{abs} 391, 640 nm.

12-Acetyl-17,18-dihydro-18,18-dimethylporphyrin (H_2C-A^{12}). Following a procedure for acetylation of aromatic compounds via Stille coupling[45] with modification, a mixture of **H_2C-Br^{12}** (14 mg, 0.034 mmol), tributyl(1-ethoxyvinyl)tin (45.0 μL, 0.134 mmol), and $(PPh_3)_2PdCl_2$ (4 mg, 0.005 mmol) was heated in acetonitrile/DMF [3 mL, (3:2)] at 85 °C for 2.5 h. The reaction mixture was treated with 10% aqueous HCl (3 mL) at room temperature for 40 min and then diluted with CH_2Cl_2. The organic phase was washed with saturated aqueous $NaHCO_3$, water, and brine. The organic layer was dried (Na_2SO_4), concentrated, and chromatographed [silica, CH_2Cl_2] to afford a purple solid (10 mg, 78%): ^{1}H NMR δ −2.29 (br s, 1H), −2.08 (br s, 1H), 2.05 (s, 6H), 3.27 (s, 3H), 4.59 (s, 2H), 8.93 (s, 1H), 8.98 (d, J = 4.5 Hz, 1H), 8.99 (d, J = 4.1 Hz, 1H), 9.01 (s, 1H), 9.13 (d, J = 4.1 Hz, 1H), 9.20 (d, J = 4.5 Hz, 1H), 9.24 (s, 1H), 9.73 (s, 1H), 10.80 (s, 1H); LD-MS obsd 381.6; ESI-MS obsd 383.1869 $(M + H)^+$ corresponds to 382.1797 (M), calcd 382.1794 ($C_{24}H_{22}N_4O$); λ_{abs} 414, 662 nm.

Zn(II)-12-acetyl-17,18-dihydro-18,18-dimethylporphyrin (ZnC-A^{12}). A solution of **H_2C-A^{12}** (9 mg, 0.02 mmol) in $CHCl_3$ (4 mL) was treated with a solution of $Zn(OAc)_2 \cdot 2H_2O$ (78 mg, 0.35 mmol) in MeOH (1 mL). The reaction mixture was stirred for 6 h at room temperature. Then the reaction mixture was concentrated, and the crude solid was dissolved in CH_2Cl_2. The organic phase was washed with saturated aqueous $NaHCO_3$, water, and brine. The organic layer was dried (Na_2SO_4) and concentrated. The solid was washed three times with hexanes. The solid was dissolved in CH_2Cl_2 (1 mL), and hexanes (1 mL) was added. The resulting precipitate was isolated by centrifugation (9 mg, 80%): ^{1}H NMR (THF-d_8) δ 2.05 (s, 6H), 3.14 (s, 3H), 4.56 (s, 2H), 8.70 (s, 1H), 8.74 (s, 1H), 8.79−8.80 (m, 1H), 8.92−8.93 (m, 1H), 9.05−9.08 (m, 2H), 9.28 (s, 1H), 9.58 (s, 1H), 10.77 (s, 1H); LD-MS obsd 444.1; ESI-MS obsd 444.0928 (M^+) corresponds to 444.0934 (M), calcd 444.0929 ($C_{24}H_{20}N_4OZn$) λ_{abs} 418, 637 nm.

12-Acetyl-15-bromo-17,18-dihydro-18,18-dimethylporphyrin (H_2C-A^{12}Br^{15}). A solution of **H_2C-A^{12}** (14.0 mg, 0.0368 mmol) in CH_2Cl_2/TFA [18 mL (10:1)] was treated with NBS (368 μL, 0.100 M in CH_2Cl_2, 0.037 mmol). The reaction mixture was stirred for 1 h at room temperature. CH_2Cl_2 was added, and the mixture was washed with $NaHCO_3$. The organic layer was dried (Na_2SO_4), concentrated, and chromatographed [silica, CH_2Cl_2/hexanes (2:1)] to afford a purple solid (7 mg, 40%): ^{1}H NMR δ −1.99 (br s, 2H), 2.03 (s, 6H), 3.25 (s, 3H), 4.58 (s, 2H), 8.75 (s, 1H), 8.76 (d, J = 4.2 Hz, 1H), 8.87 (d, J = 4.8 Hz, 1H), 8.95 (d, J = 4.2 Hz, 1H), 9.06 (d, J = 4.8 Hz, 1H), 9.44 (s, 1H), 9.48 (s, 1H), 10.63 (s, 1H); MALDI-MS obsd 460.3; ESI-MS obsd 461.09692 $(M + H)^+$ corresponds to 460.08965 (M), calcd 460.08987 ($C_{24}H_{21}BrN_4O$); λ_{abs} 418, 664 nm.

2-Bromodipyrromethane (5). A solution of **4** (2.48 g, 14.4 mmol) in anhydrous THF/methanol (144 mL) at 0 °C was slowly treated with $NaBH_4$ (8.85 g, 233 mmol) in portions. The mixture was stirred for 2 h. Then water and ethyl acetate were added, and the resulting mixture was stirred for 20 min. After thorough extraction with ethyl acetate, the organic layer was separated, dried (Na_2SO_4), and concentrated to give a colorless oil, which was used in the next stage without purification. The oil was dissolved in pyrrole (20.0 mL, 287 mmol). The solution was degassed with a stream of argon for 10 min and then treated with $InCl_3$ (343 mg, 1.55 mmol). The mixture was stirred overnight under argon. The mixture turned dark brown during the first hour of reaction. The reaction mixture was quenched with 1 M NaOH (50 mL). After extraction with ethyl acetate, the organic layer was dried (Na_2SO_4) and concentrated. The excess pyrrole was recovered under high vacuum. The resulting crude brown oil was chromatographed [silica, hexanes/CH_2Cl_2/ethyl acetate (7:2:1)] to afford a pale yellow oil that turned brown upon storage (2.02 g, 58%): ^{1}H NMR δ 3.89 (s, 2H), 6.02−6.03 (m, 2H), 6.13−6.16 (m, 1H),

6.58−6.59 (m, 1H), 6.65−6.66 (m, 1H), 7.66−7.84 (br s, 2H); ^{13}C NMR δ 26.5, 96.1, 107.1, 108.7, 109.2, 117.2, 117.9, 128.2, 130.2; ESI-MS obsd 225.00137 $(M+H)^+$ corresponds to 223.99409 (M), calcd 223.99491 ($C_9H_9BrN_2$).

8-Bromo-1-formyldipyrromethane (1-Br^8). A sample of DMF (7.00 mL) was treated with $POCl_3$ (1.00 mL, 10.9 mmol) at 0 °C under argon, and the mixture was stirred for 10 min. Then a solution of **5** (1.94 g, 8.55 mmol) in DMF (25 mL) at 0 °C was treated with the freshly prepared Vilsmeier reagent (5.62 mL) under argon. The resulting mixture was stirred for 2 h at 0 °C. The mixture was poured into a cooled mixture of 2 M NaOH (120 mL) and CH_2Cl_2 (80 mL) at 0 °C and stirred for 20 min. The organic phase was washed (saturated aqueous NH_4Cl, water, and brine), dried (Na_2SO_4), and concentrated to give a red-brownish oil. The oil was treated with hexanes and concentrated to give a brown solid. Column chromatography [silica, hexanes/ethyl acetate (6:1)] afforded a brown solid. For recrystallization the solid was dissolved in the minimal amount of warm CH_2Cl_2, which upon cooling afforded pale brown crystals (868 mg, 40%): mp 134−135 °C dec; ^{1}H NMR (acetone-d_6) δ 4.02 (s, 2H), 5.93−5.95 (m, 1H), 6.08−6.09 (m, 1H), 6.73−6.75 (m, 1H), 6.89−6.90 (m, 1H), 9.41 (s, 1H), 10.6 (br s, 1H), 10.9 (br s, 1H); ^{13}C NMR (acetone-d_6) δ 27.2, 96.2, 110.0, 110.8, 118.4, 122.4, 131.0, 134.1, 140.6, 179.2; ESI-MS obsd 252.99694 $(M+H)^+$ corresponds to 251.98966 (M), calcd 251.98983 ($C_{10}H_9BrN_2O$). Anal. Calcd for $C_{10}H_9BrN_2O$: C, 47.46; H, 3.58; N, 11.07. Found: C, 47.74, H, 3.52, N, 11.03.

8,9-Dibromo-1-formyldipyrromethane (1-Br^{8,9}). A solution of **1-Br^8** (506 mg, 2.00 mmol) in anhydrous THF (20 mL) was treated with NBS (356 mg, 2.00 mmol) in one batch under argon at −78 °C. The reaction mixture was stirred for 1 h at −78 °C, after which the ice bath was removed, and the reaction mixture was allowed to warm up. Upon reaching 5 °C, hexanes and water were added. The mixture was extracted with ethyl acetate. The organic layer was dried (K_2CO_3) and concentrated to afford a brown solid. The solid was suspended in warm CH_2Cl_2, and THF was added to achieve complete dissolution, whereupon hexanes was added. Pale yellow crystals were obtained (476 mg, 71%): mp 104−105 °C dec; ^{1}H NMR (acetone-d_6) δ 4.03 (s, 2H), 6.03 (s, 1H), 6.10 (d, J = 3.9 Hz, 1H), 6.89 (d, J = 3.9 Hz, 1H), 9.41 (s, 1H), 10.9 (br s, 1H), one NH was not observed presumably due to deuterium exchange; ^{13}C NMR (acetone-d_6) δ 27.2, 98.2, 98.8, 110.7, 111.0, 122.4, 132.2, 133.8, 139.9, 179.1; ESI-MS obsd 330.90857 $(M+H)^+$ corresponds to 329.90130 (M), calcd 329.90034 ($C_{10}H_8Br_2N_2O$). Anal. Calcd for $C_{10}H_8Br_2N_2O$: C, 36.18; H, 2.43; N, 8.44. Found: C, 36.08, H, 2.43, N, 8.28.

Zn(II)-3,13-dibromo-17,18-dihydro-18,18-dimethylporphyrin (ZnC-Br^{3}Br^{13}). A solution of **1-Br^{8,9}** (134 mg, 0.400 mmol) and **6** (107 mg, 0.400 mmol) in anhydrous CH_2Cl_2 (10.6 mL) was treated with a solution of $TsOH\cdot H_2O$ (380 mg, 2.00 mmol) in anhydrous methanol (2.8 mL) under argon. The reaction mixture changed immediately to orange-red. The mixture was stirred for 30 min under argon, then treated with 2,2,6,6-tetramethylpiperidine (746 μL, 4.40 mmol) and concentrated to dryness. The resulting brown solid was suspended in acetonitrile (40 mL), and 2,2,6,6-tetramethylpiperidine (1.70 mL, 10.0 mmol), $Zn(OAc)_2$ (1.10 g, 6.00 mmol), and AgOTf (308 mg, 1.20 mmol) were added consecutively. The resulting suspension was refluxed for 22 h exposed to air. The crude mixture was filtered through a silica pad with CH_2Cl_2, and the filtrate was chromatographed [silica, CH_2Cl_2] to afford a green solid (21 mg, 9%): ^{1}H NMR (THF-d_8) δ 2.04 (s, 6H), 4.61 (s, 2H), 8.65 (s, 1H), 8.86−8.87 (m, 2H), 8.95 (d, J = 4.1 Hz, 1H), 9.01 (d, J = 4.1 Hz, 1H), 9.14 (s, 1H), 9.57 (s, 1H), 9.73 (s, 1H); ^{13}C NMR (THF-d_8) δ 31.5, 46.4, 51.7, 94.0, 95.1, 109.1, 109.2, 115.8, 128.6, 129.4, 129.8, 133.0, 133.7, 144.6, 147.6, 147.8, 148.3, 149.3, 155.1, 159.8, 171.6; MALDI-MS obsd 557.9; ESI-MS obsd 557.9021 (M^+) corresponds to 557.90238, calcd 557.90330 ($C_{22}H_{16}Br_2N_4Zn$); λ_{abs} 405, 619 nm.

Zn(II)-13-bromo-17,18-dihydro-18,18-dimethyl-3-[2-(triisopropylsilyl)ethynyl]porphyrin (ZnC-E^{3}Br^{13}). A solution of **1-Br^{8,9}** (117 mg, 0.350 mmol) and **7** (130 mg, 0.350 mmol) in anhydrous CH_2Cl_2 (10.0 mL) was treated with a solution of $TsOH\cdot H_2O$ (333 mg, 1.75 mmol) in anhydrous methanol (2.5 mL) under argon. The reaction mixture changed immediately to orange-red. The mixture was stirred for 40 min under argon, then treated with 2,2,6,6-tetramethylpiperidine (655 μL, 3.85 mmol) and concentrated to dryness. The resulting light brown solid was suspended in acetonitrile (35 mL), and the mixture was placed in an 80 mL pressurized microwave flask. The microwave apparatus has been described.[34] 2,2,6,6-Tetramethylpiperidine (1.48 mL, 8.75 mmol), $Zn(OAc)_2$ (966 mg, 5.25 mmol), and AgOTf (270 mg, 1.05 mmol) were added consecutively to the solution. The flask was inserted in a microwave reactor, and the reaction was carried out at 81 °C for 1.5 h. The crude mixture was filtered through a silica pad with ethyl acetate, and the filtrate was concentrated and chromatographed [silica, CH_2Cl_2/hexanes (3:2)] to afford a dark green solid (11 mg, 5%): ^{1}H NMR (THF-d_8) δ 1.44−1.46 (m, 21H), 2.04 (s, 6H), 4.62 (s, 2H), 8.67 (s, 1H), 8.86 (s, 1H), 8.91 (s, 1H), 8.95 (s, 1H + 1H), 9.14 (s, 1H), 9.56 (s, 1H), 9.87 (s, 1H); ^{13}C NMR (THF-d_8) δ 12.7, 19.5, 31.3, 46.1, 51.6, 94.2, 95.3, 98.8, 104.4, 106.7, 108.6, 116.5, 127.0, 130.0, 130.2, 130.7, 133.2, 145.3, 147.3, 147.9, 148.5, 149.5, 152.5, 160.3, 171.3; MALDI-MS obsd 660.4; ESI-MS obsd 660.1261 (M^+) corresponds to 660.1255 (M), calcd 660.1262 ($C_{33}H_{37}BrN_4SiZn$); λ_{abs} 412, 632 nm.

Zn(II)-17,18-dihydro-18,18-dimethyl-3,13-bis[2-(triisopropylsilyl)ethynyl]porphyrin (ZnC-E^{3}E^{13}). Following a procedure for ethynylation of chlorins via Sonogashira coupling,[26] a mixture of **ZnC-Br^{3}Br^{13}** (38 mg, 0.068 mmol), (triisopropylsilyl)acetylene (95 μL, 0.41 mmol), $Pd_2(dba)_3$ (19 mg, 0.020 mmol), and P(*o*-tol)$_3$ (50 mg, 0.16 mmol) was heated in toluene/triethylamine [12 mL, (3:1)] at 60 °C for 8 h, using a Schlenk line. The reaction mixture was concentrated and chromatographed [silica, hexanes/CH_2Cl_2 (3:1)] to afford a green solid (18 mg, 35%): ^{1}H NMR (THF-d_8) δ 1.43−1.46 (m, 42H), 2.06 (s, 6H), 4.60 (s, 2H), 8.64 (s, 1H), 8.91 (s, 1H), 8.93 (d, J = 4.2 Hz, 1H), 8.96 (d, J = 4.2 Hz, 1H), 9.03 (s, 1H), 9.18 (s, 1H), 9.58 (s, 1H), 9.85 (s, 1H); ^{13}C NMR (THF-d_8) δ 12.7, 13.0, 19.1, 19.5, 31.4, 46.2, 51.5, 94.8, 95.0, 97.5, 98.8, 104.4, 104.7, 106.4, 109.4, 122.1, 127.0, 130.1, 130.8, 135.5, 145.7, 147.5, 148.2, 148.7, 152.7, 153.7, 160.2, 171.6, one α-carbon was not observed owing to overlap; MALDI-MS obsd 762.8; ESI-MS obsd 763.3585 $(M+H)^+$ corresponds to 762.35122 (M), calcd 762.34915 ($C_{44}H_{58}N_4Si_2Zn$); λ_{abs} 416, 643 nm; λ_{em} (λ_{ex} = 416 nm) 644 nm.

Zn(II)-13-acetyl-17,18-dihydro-18,18-dimethyl-3-[2-(triisopropylsilyl)ethynyl]porphyrin (ZnC-E^{3}A^{13}). The following procedure entails zinc demetalation, Pd-mediated coupling with tributyl(1-ethoxyvinyl)tin, acidic hydrolysis, and zinc metalation. A solution of **ZnC-E^{3}Br^{13}** (18 mg, 0.027 mmol) in CH_2Cl_2 (1 mL) was treated dropwise with TFA (42 μL, 0.54 mmol). After 5 h CH_2Cl_2 was added, and the organic layer was washed (saturated aqueous $NaHCO_3$, water, brine), dried (Na_2SO_4), and concentrated. The resulting crude solid was used in the next step. A mixture of crude solid, tributyl(1-ethoxyvinyl)tin (0.037 mL, 0.11 mmol), and $(PPh_3)_2PdCl_2$ (3 mg, 0.004 mmol) was stirred in acetonitrile/DMF [2.5 mL, (3:2)] at 85 °C, using a Schlenk line. After 3.5 h the reaction mixture was treated with 10% aqueous HCl (3.5 mL) at room temperature. The mixture was stirred for 1 h. CH_2Cl_2 was added, and the organic layer was washed (saturated aqueous $NaHCO_3$, water, brine), dried (Na_2SO_4), and concentrated. The crude solid was dissolved in $CHCl_3$ (4 mL), and the solution was treated with $Zn(OAc)_2\cdot 2H_2O$ (89 mg, 0.41 mmol) in MeOH (1 mL). The reaction

mixture was stirred for 16 h at room temperature. Then the reaction mixture was concentrated and chromatographed [silica, CH_2Cl_2/hexanes (2:1)] to afford a green solid (10 mg, 59%): ^{1}H NMR (THF-d_8) δ 1.43 (s, 21H), 2.02 (s, 6H), 3.09 (s, 3H), 4.56 (s, 2H), 8.58 (s, 1H), 8.87 (s, 1H), 8.88 (d, J = 3.9 Hz, 1H), 8.95 (d, J = 3.9 Hz, 1H), 9.63 (s, 1H), 9.64 (s, 1H), 9.75 (s, 1H), 9.88 (s, 1H); ^{13}C NMR (THF-d_8) δ 12.7, 19.5, 29.6, 31.2, 46.2, 51.5, 95.0, 98.7, 99.1, 104.2, 105.8, 111.4, 127.5, 130.0, 130.7, 131.7, 135.2, 138.3, 143.5, 148.35, 148.42, 149.3, 150.8, 153.6, 160.4, 172,5, 196.0; MALDI-MS obsd 624.8; ESI-MS obsd 625.2320 $(M+H)^+$ corresponds to 624.22476 (M), calcd 624.22628 ($C_{35}H_{40}N_4OSiZn$); λ_{abs} 420, 645 nm; λ_{em} (λ_{ex} = 420 nm) 650 nm.

Acknowledgment. This research was supported by grants from the Chemical Sciences, Geosciences and Biosciences Division, Office of Basic Energy Sciences, Office of Science, U.S. Department of Energy to D.H. (DE-FG02-05ER15661), D.F.B. (DE-FG02-05ER15660), and J.S.L. (DE-FG02-96ER14632). Olga Mass was the recipient of a Burroughs-Wellcome Fellowship. Mass spectra were obtained at the Mass Spectrometry Laboratory for Biotechnology at North Carolina State University. Partial funding for the facility was obtained from the North Carolina Biotechnology Center and the National Science Foundation. We thank Dr. Chinnasamy Muthiah for obtaining the X-ray structures of selected chlorins.

Supporting Information Available: Spectral data (^{1}H NMR and ^{13}C NMR) for all new chlorins including spectral assignments; additional information concerning experimental procedures; X-ray data for four chlorins and one 13^1-oxophorbine (**H_2C-A^{12}Br^{15}**, **ZnC-Br^{3}Br^{13}**, **ZnC-T^{5}M^{10}A^{13}**, **ZnC-M^{10}Br^{13}**, **H_2OP-T^{5}M^{10}**). This material is available free of charge via the Internet at http://pubs.acs.org.